Alzheimer's & Dementia: Translational Research & Clinical Interventions 4 (2018) 89-102

Featured Article

Elevated phospholipase D isoform 1 in Alzheimer's disease patients' hippocampus: Relevance to synaptic dysfunction and memory deficits

Balaji Krishnan*, Rakez Kayed, Giulio Taglialatela

UTMB Mitchell Center for Neurodegenerative Diseases, Department of Neurology, University of Texas Medical Branch, Galveston, TX, USA

Abstract

Introduction: Phospholipase D (PLD), a lipolytic enzyme that breaks down membrane phospholipids, is also involved in signaling mechanisms downstream of seven transmembrane receptors. Abnormally elevated levels of PLD activity are well-established in Alzheimer's disease (AD), implicating the two isoforms of mammalian phosphatidylcholine cleaving PLD (PC-PLD1 and PC-PLD2). Therefore, we took a systematic approach of investigating isoform-specific expression in human synaptosomes and further investigated the possibility of therapeutic intervention using preclinical studies.

Methods: Synaptosomal Western blot analyses on the postmortem human hippocampus, temporal cortex, and frontal cortex of AD patient brains/age-matched controls and the 3XTg-AD mice hippocampus (mouse model with overexpression of human amyloid precursor protein, presenilin-1 gene, and microtubule-associated protein tau causing neuropathology progressing comparable to that in human AD patients) were used to detect the levels of neuronal PLD1 expression. Mouse hippocampal long-term potentiation of PLD1-dependent changes was studied using pharmacological approaches in *ex vivo* slice preparations from wild-type and transgenic mouse models. Finally, PLD1-dependent changes in novel object recognition memory were assessed following PLD1 inhibition.

Results: We observed elevated synaptosomal PLD1 in the hippocampus/temporal cortex from postmortem tissues of AD patients compared to age-matched controls and age-dependent hippocampal PLD1 increases in 3XTg-AD mice. PLD1 inhibition blocked effects of oligomeric amyloid β or toxic oligomeric tau species on high-frequency stimulation long-term potentiation and novel object recognition deficits in wild-type mice. Finally, PLD1 inhibition blocked long-term potentiation deficits normally observed in aging 3XTg-AD mice.

Discussion: Using human studies, we propose a novel role for PLD1-dependent signaling as a critical mechanism underlying oligomer-driven synaptic dysfunction and consequent memory disruption in AD. We, further, provide the first set of preclinical studies toward future therapeutics targeting PLD1 in slowing down/stopping the progression of AD-related memory deficits as a complementary approach to immunoscavenging clinical trials that are currently in progress.

Keywords: Phospholipase D; Alzheimer's disease; Memory; Synaptic; Hippocampus; Electrophysiology; Novel object recognition; Aβ; Tau

1. Introduction

Alzheimer's disease (AD), the most common form of dementia, is the fifth leading cause of death in America [1]. Therapeutic strategies, based on the last 3 decades of research, have largely targeted accumulations of oligomeric amyloid β (oAβ) [2] and oligomeric tau species (otau) [3]. Clinical trials that target these aggregates alone have not enjoyed as much success [4,5]. Thus, recent studies have also started to identify other players in the early events, such as synapse dysfunction [6,7].

In the present study, we systematically addressed the role of phospholipase D (PLD) in early events leading to synaptic vulnerability. PLD enzyme superfamily members are transphosphatidylases that conduct headgroup exchange on phosphatidic acid at the terminal phosphodiester bond [8]. In addition, PLD signaling is important for several physiological

The authors declare no competing financial interests.

*Corresponding author. Tel.: 409 772 8069; Fax: 409 747 0015.
E-mail address: bakrishn@utmb.edu

https://doi.org/10.1016/j.trci.2018.01.002

processes including membrane trafficking, cytoskeletal reorganization, and autophagy that is regulated upstream by several transmembrane receptors including G-protein-coupled receptors, receptor tyrosine kinases, and integrin receptors [9,10]. In fact, our previous studies show that PLD isoforms can act as convergent second messengers for dopaminergic, serotonergic, and glutamatergic neurotransmission [11–13] affecting synaptic function and memory processes.

Mammalian phosphatidylcholine cleaving PLD (two isoforms: PLD1 and PLD2) cleaves phosphatidylcholine to phosphatidic acid/choline via phosphodiesterase action, and brain-associated PLD function can affect membrane curvature, exocytosis, endocytosis, vesicle release, and neurite outgrowth, all of which are important in synaptic function [9]. Our previous studies also implicated PLD isoforms in rodent associative memory mechanisms [11–13].

Evidence for aberrant increase in PLD activity in postmortem AD brains, compared to controls, arrived nearly 3 decades ago [14]. Mouse studies implicating PLD2 (the constitutive isoform) in Aβ-driven synaptic dysfunction [15] were not validated by confirming that an increased expression of PLD2 in postmortem AD brains, indeed, contributes to the neuropathology of AD-like memory deficits. Attention to the possibility of PLD1 (the inducible isoform) contributing to AD synaptic dysfunction was completely disregarded.

A role for PLD1 in AD, done exclusively in cell culture, proposed a protective role for PLD1 against Aβ synthesis [16,17], which is confounded by a study in humans that shows that there is upregulated astroglial PLD1 expression in AD brains [18] but does not result in any neuroprotection. Thus, a clearer role for PLD isoforms in AD requires an approach that starts with addressing the relative levels of neuronal PLD1 and PLD2 expression in normal and diseased states in the human brain.

Here, we report, for the first time, a systematic study demonstrating the relative synaptosomal expression levels of the two phosphatidylcholine cleaving PLD isoforms in postmortem control and AD brains. Furthermore, we extended our observation to study whether inhibition of PLD isoforms via specific small molecule inhibitors [8] prevents synaptic dysfunction and memory defects of Aβ and tau oligomers in wild-type mice using electrophysiology and behavior, respectively. In addition, we also addressed whether the convergent synaptic deficits induced by overexpression of human genes for amyloid precursor protein (APP) and tau in the 3XTg-AD mice (mouse model with overexpression of human APP, presenilin-1 gene, and microtubule-associated protein tau) [19] were attenuated by inhibiting PLD1 signaling.

2. Materials and methods

2.1. Human subjects and autopsy brain tissues

Postmortem de-identified brain tissues were obtained through materials transfer agreement from Oregon Brain Bank at Oregon Health and Science University, Portland, OR. After obtaining informed consent, enrolled donor subjects were clinically evaluated in accordance with Oregon Brain Bank at Oregon Health and Science University's, Portland, OR, institutional review board–approved protocols. A neuropathological assessment was performed at autopsy for amyloid plaques and neurofibrillary tangles, per standardized Consortium to Establish a Registry for Alzheimer's Disease criteria and Braak staging. Participants were classified as AD (n = 11) when possessing Mini–Mental State Examination score below 10. Control participants (n = 8) performed normally (Mini–Mental State Examination of 28–30). Donor subject samples were de-identified before arrival at University of Texas Medical Branch. The clinical data of the subjects used in the study are provided in Table 1.

2.2. Western blot analysis

Isolation of synaptosomal fractions from the frozen brain sections (hippocampus, frontal cortex, and temporal cortex) obtained from different groups as mentioned previously was performed using the Syn-PER reagent (Thermo Fisher Scientific, Waltham, MA) according to the manufacturer's protocol. The Syn-PER reagent with protease and phosphatase inhibitors, to prevent protein degradation, was used at 1 mL per 100 mg of brain tissue. Following 10 strokes using the dounce homogenizer, the brain tissue suspension in Syn-PER was subjected to 1200× *g* for 10-minute centrifugation. The supernatant fraction was then further centrifuged at

Table 1
Diagnosis of the de-identified subjects based on Braak staging of plaques and tangles localization [20,21] and MMSE

Diagnosis	Subject number	Age	Sex	Braak stage	MMSE	PMI
Ctrl	767	86	F	2	-	8
Ctrl	785	82.7	M	1	-	<14
Ctrl	1957	>89	F	4	30	8
Ctrl	1977	92	F	4	-	4
Ctrl	1874	43	F	0	-	10
Ctrl	1876	28	F	0	-	15.5
Ctrl	1899	79	F	2	25	14
Ctrl	2229	71	F	2	-	14.5
AD	1538	84	M	5	26	5.5
AD	1749	79	?	6	-	6
AD	1756	68	M	6	7	11.5
AD	1766	63	F	6	18	3.5
AD	1776	>89	F	6	6	6.3
AD	1777	67	F	6	9	20.5
AD	1910	63	F	6	-	44
AD	1985	?	?	-	-	-
AD	2201	86	M	6	-	16
AD	2316	83	M	5	-	11
AD	2317	88	M	6	-	4

Abbreviations: AD, Alzheimer's disease; Ctrl, control; F, female; M, male; MMSE, Mini–Mental State Examination; PMI, post-mortem interval.

NOTE. PMI provides the postmortem interval for brain removal after death of the subject in hours. As indicated, samples from either sex were used for the study, where Braak stage of 5 and more with MMSE (for those available) 24 and below are diagnosed as AD, whereas the others were selected as the control group.

15,000× g for 20 minutes. All procedures were conducted at 4°C. The resulting pellet containing the synaptosomes was resuspended in HEPES-buffered Krebs-like buffer. Bicinchoninic acid assay (Thermo Fisher Scientific) was used for determining protein concentrations, and Western blot analysis was performed as described previously [22]. If stored at −80°C until further use, dimethyl sulfonic acid (final concentration of 5%) was added to the synaptosomes. Thawing the synaptosomes was done by placing the tubes at 37°C for 5 minutes, adding twice the volume of cold HEPES-buffered Krebs-like buffer, centrifuged at 15,000× g for 10 minutes at 4°C and then resuspended the ensuing synaptosomal pellet in fresh cold HEPES-buffered Krebs-like buffer.

2.3. Antibodies

Primary antibodies include Phospho-PLD1 at threonine 147 (rabbit polyclonal, pPLD1T147-3831, 1:1000; Cell Signaling Technology, Danvers, MA), PLD1 (rabbit polyclonal, H-160 sc-25512, 1:100; Santa Cruz Technologies, Santa Cruz, CA), PLD2 (rabbit polyclonal, H-133 sc-25513, 1:100; Santa Cruz), and β-actin (mouse monoclonal, MAB1501, 1:5000; Chemicon International, Temecula, CA). Secondary antibodies include goat anti-mouse (IRDye 680; 926–32,220, 1:10,000; LI-COR Biosciences, Lincoln, NE) and goat anti-rabbit (IRDye 800; 827–08,365, 1:10,000; LI-COR Biosciences).

2.4. Data analysis for Western blots

Membranes were imaged using the Odyssey Infrared Imaging System (LI-COR Biosciences) at 700 and/or 800 nm at 169-μm resolution. The integrated intensity of each band was analyzed with the Odyssey Infrared Imaging System Application, version 2.1, Software. The ratio of PLD band intensity to β-actin band intensity was determined for each sample for normalization.

2.5. Animals

C57Bl/6 male and female mice (2–6 months of age, n = 110) were purchased from Jackson Labs (Bar Harbor, ME). All animals were acclimated in a colony room at a constant temperature (21–23°C) and humidity (45–50%) on a 12-: 12-hour light-dark cycle (lights on 6:00 am–6:00 pm) and housed five per cage with chow and water *ad libitum*. Male and female 3XTg-AD [19] transgenic mice were purchased from Jackson Labs and maintained (n = 36 animals including wild-type siblings) through a breeding program at University of Texas Medical Branch. The study was approved by the University of Texas Medical Branch Institutional Animal Care and Use Committee as per the National Institutes of Health Guidelines [23] on the use of laboratory animals.

2.6. Drugs

Human $A\beta_{1–42}$ was purchased (Department of Biophysics and Biochemistry, Harvard University, MA), and oligomers were prepared as described previously [24]. Biologically relevant tau oligomers from biological samples were prepared and characterized as described previously [25]. PLD1 inhibitor (VU0155069) and PLD2 inhibitor (VU0364739) were obtained from Tocris Bioscience (Bio-Techne, Minneapolis, NE). Treatment with oligomers/inhibitors on *ex vivo* slices and behavior is described below.

2.7. Field excitatory postsynaptic potential recordings

Acute brain slice methods described earlier [26] were modified [27]. Briefly, mice were deeply anesthetized with isoflurane and transcardially perfused with 25 to 30 mL of carbogenated (95% O_2 and 5% CO_2 gas mixture) N-methyl-D-gluconate-artificial cerebrospinal fluid at room temperature. Transverse brain sections of 350 μm containing Schaffer collateral synapses were generated using the Compresstome VF-300 (Precisionary Instruments, Greenville, NC). An initial protective recovery was done in the cutting solution at 32°C–34°C for <12 minutes and then transferred to carbogen bubbling HEPES-artificial cerebrospinal fluid recovery solution at room temperature. After recovery, slices were perfused in carbogen bubbling room temperature normal artificial cerebrospinal fluid at a rate of approximately 3 mL/min. Treatments with oligomers (prepared as described in Section 2.6) occurred in the recovery phase where the slices were isolated to a separate chamber and incubated with the desired concentration of the oligomers for 1 hour. Slice treatment with a PLD inhibitor was done for 1 hour and 15 minutes. For the dual oligomer-inhibitor treatment, the inhibitor was added 15 minutes before the addition of the oligomer (see schematics provided in Figs. 1–3). After the treatment, the slices were briefly washed by placing them in drug-free, oligomer-free recovery artificial cerebrospinal fluid for 5 minutes before placing them on the recording stage. Using a horizontal P-97 Flaming/Brown micropipette puller (Sutter Instruments, Novato, CA), borosilicate glass capillaries were used to pull electrodes and filled with normal artificial cerebrospinal fluid to get a resistance of 1–2 MΩ. Evoked field excitatory postsynaptic potentials (fEPSPs) in the CA1 by stimulating Schaffer collateral were measured using high-frequency stimulation (HFS; 3 × 100 Hz, 20 seconds) as described in our previous studies [24,28], digitized using Digidata 1550B (Molecular Devices, Sunnyvale, CA), and collected using an Axon MultiClamp 700B differential amplifier (Molecular Devices) connected to a Windows 7 computer (Dell Instruments, Round Rock, TX) running Clampex 10.6 software (Molecular Devices). Current stimulation was delivered through a digital stimulus isolation amplifier (A.M.P.I., Israel) and set to elicit an fEPSP approximately 30% of maximum for synaptic potentiation experiments using platinum iridium–tipped concentric bipolar electrodes (FHC Inc., Bowdoin, ME). A stable baseline was obtained by delivering single-pulse stimulation at 20-second interstimulus intervals. All data are represented as percentage

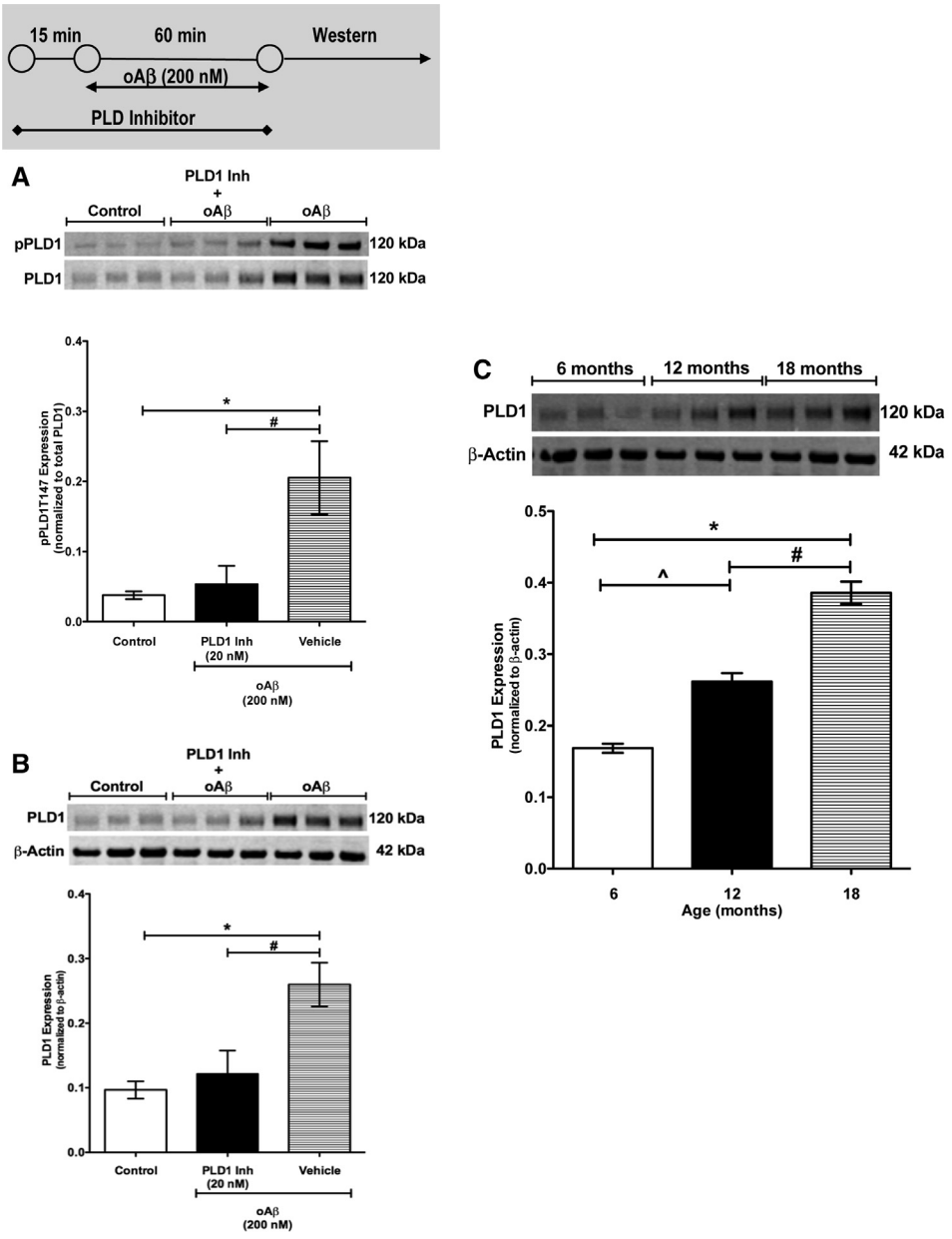

Fig. 1. PLD1 expression and activity in the mouse hippocampus increases following acute oAβ treatment, and in addition, synaptosomal PLD1 expression shows an age-dependent increase in the 3XTg-AD mouse hippocampus. (A) Phosphorylated PLD1 levels (control [hollow bars]: 0.038 ± 0.006, n = 3; PLD1 inhibitor + oAβ [black bars]: 0.054 ± 0.026, n = 3; and vehicle + oAβ [horizontal bars]: 0.205 ± 0.005, n = 3) and (B) synaptosomal PLD1 levels (control [hollow bars]: 0.097 ± 0.013, n = 3; PLD1 inhibitor + oAβ [black bars]: 0.121 ± 0.036, n = 3; and vehicle + oAβ [horizontal bars]: 0.260 ± 0.034, n = 3) are increased following acute application of oAβ in WT mouse hippocampi compared to controls. (C) An age-dependent increase in hippocampal synaptosomal PLD1 expression (6 months [hollow bars]: 0.168 ± 0.006, n = 3; 12 months [black bars]: 0.262 ± 0.012, n = 3; and 18 months [horizontal bars]: 0.386 ± 0.016, n = 3) is also observed in the 3XTg-AD mouse model. Each lane in the blots above the graph represents the protein sample from one animal. A minimum of three mice were tested per condition. * indicates $P < .05$ compared to the control group, whereas ^ indicates $P < .05$ between 6- and 12-month-old 3XTg-AD female mice (C). # indicates $P < .05$ compared to the PLD1 inhibitor + ACSF application group (B) and between 12- and 18-month-old 3XTg-AD female mice (C). Statistical significance was assessed using nonparametric analysis to account for the sample size and distribution using Mann-Whitney *U* post hoc analysis. Abbreviations: 3XTg-AD, mouse model with overexpression of human amyloid precursor protein, presenilin-1 gene, and microtubule-associated protein tau; Aβ, amyloid β; ACSF, artificial cerebrospinal fluid; Inh, inhibitor; oAβ, oligomeric Aβ; PLD, phospholipase D; PLD1, phospholipase D isoform 1; pPLD1, phosphorylated PLD1.

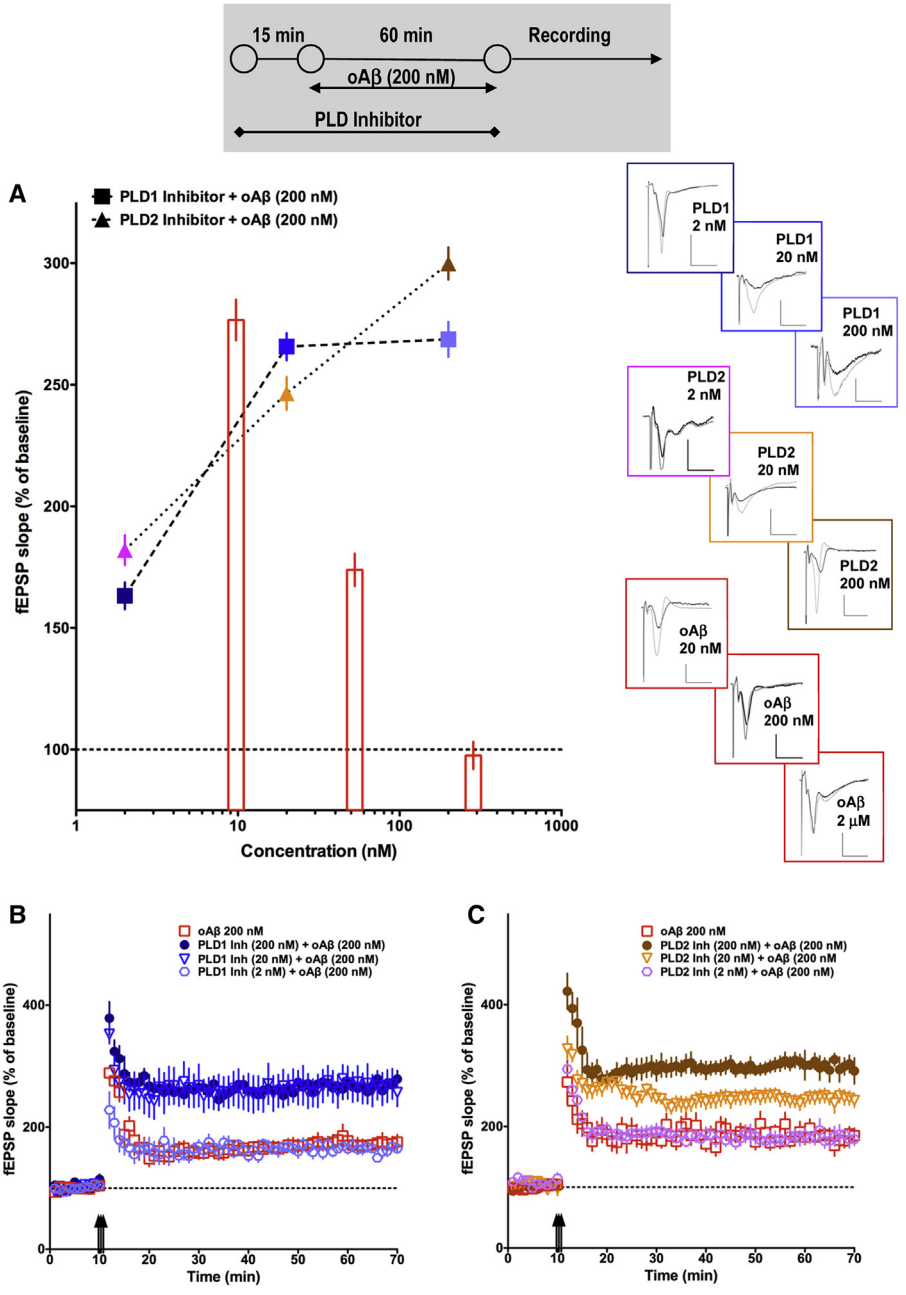

Fig. 2. Inhibiting PLD activity prevents the synaptic dysfunction driven by oAβ in the Schaffer collateral synapses in the WT mouse hippocampus. fEPSPs were evaluated following standard HFS protocol (3 × 100 Hz) depicted by three arrows in (B) and (C) and compared to the baseline and plotted as a percentage of the original value (A–C). Applications of the oligomers follow the schematic depicted in the gray box above the graphs. Representative traces are provided next to the bars or symbols, with the length of the vertical scale bar at 0.5 mV and the horizontal scale bar at 10 ms. The application of the inhibitor was started 15 minutes before the application of the oligomers and continued through the time that the slices were incubated with the oligomers. (A) As the oAβ concentration increased from 20 nM to 2 μM, the HFS LTP (last 10 minutes) decreased from ∼280% to ∼100% (clear bars—20 nM oAβ: 281.20 ± 8.515, n = 12; 200 nM oAβ: 176.10 ± 6.798, n = 24; and 2-μM oAβ: 98.09 ± 5.730, n = 12). Both PLD1-specific inhibitor (VU0155069, filled squares) and PLD2-specific inhibitor (VU0364739, filled triangles) were ineffective in suppressing the LTP effect of 200 nM oAβ at the lowest concentration tested (2 nM PLD1 inhibitor: 163.2 ± 5.509, n = 6 and 2 nM PLD2 inhibitor: 182.0 ± 6.137, n = 6) but could prevent the oAβ-driven LTP deficit at higher concentrations (20 nM PLD1 inhibitor: 265.7 ± 5.590, n = 6; 20 nM PLD2 inhibitor: 246.5 ± 6.724, n = 6; 200 nM PLD1 inhibitor: 268.7 ± 7.183, n = 6; and 200 nM PLD2 inhibitor: 299.9 ± 6.618, n = 6, $*P < .05$). (B) PLD1 inhibitor at 20 nM (inverted hollow triangles) and 200 nM (filled circles) shows complete recovery of the Schaffer collateral HFS LTP including PTP (first 10 minutes) and LTP (last 10 minutes), whereas the inhibitor at 2 nM (hollow hexagons) is ineffective in overcoming effect of oAβ inhibition (200 nM, hollow squares). (C) The PLD2 inhibitor at the highest concentration tested (200 nM, filled circles) completely attenuates the LTP deficits seen with oAβ (200 nM, hollow squares), whereas it is completely ineffective at 2 nM (hollow hexagons), with some recovery of PTP, but not LTP. At the intermediate concentration of 20 nM (inverted triangles), the PLD2 inhibitor shows an intermediate recovery of the LTP that is significantly higher than 2 nM, but lower than 200 nM. Statistical significance was assessed using nonparametric one-way ANOVA (Kruskal-Wallis test) followed by Dunn's multiple comparison. Abbreviations: Aβ, amyloid β; ANOVA, analysis of variance; fEPSP, field excitatory postsynaptic potential; HFS, high-frequency stimulation; Inh, inhibitor; LTP, long-term potentiation; oAβ, oligomeric Aβ; PLD, phospholipase D; PLD1, phospholipase D isoform 1; PLD2, phospholipase D isoform 2; PTP, posttetanic potentiation; WT, wild-type.

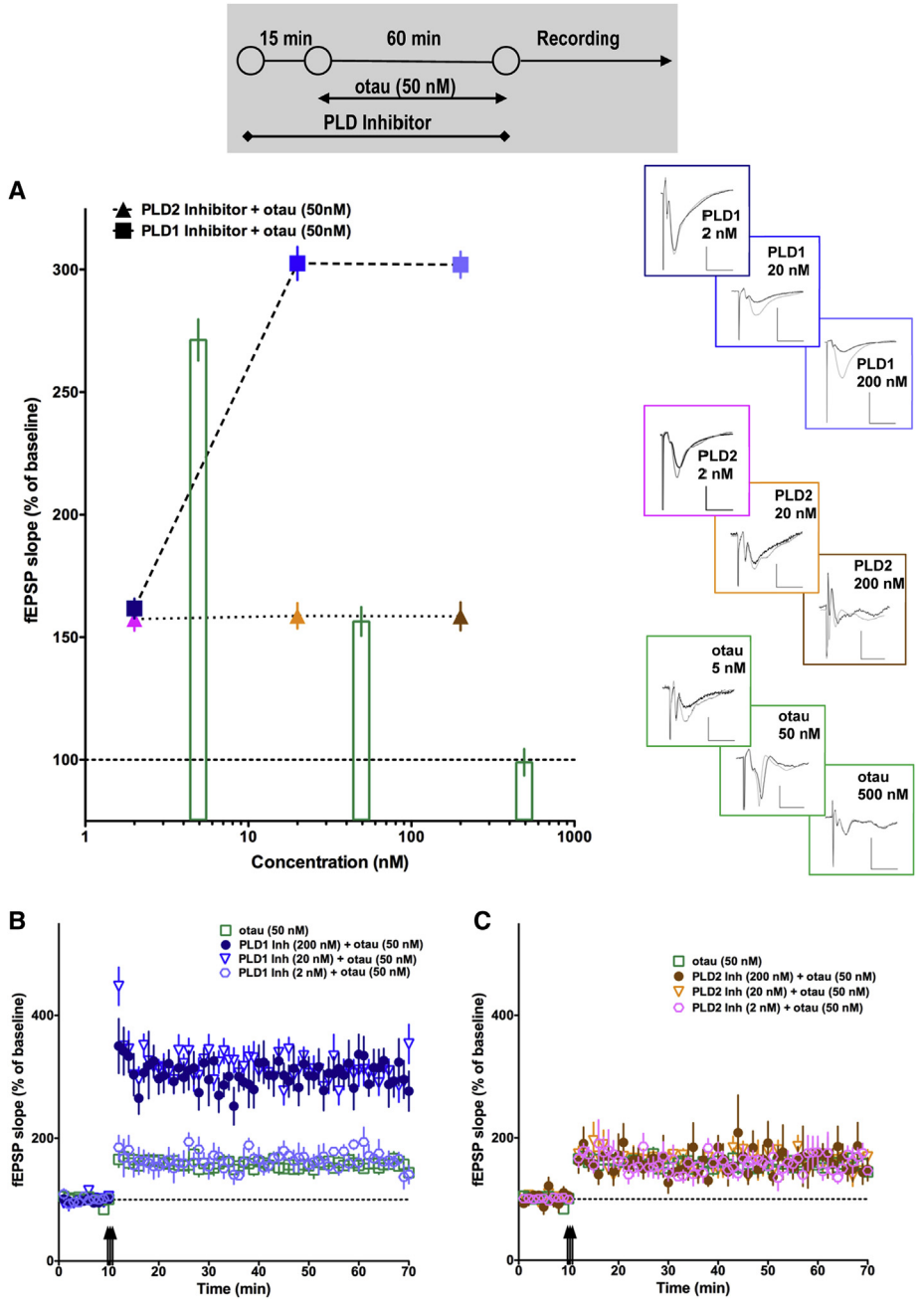

Fig. 3. Inhibiting PLD1 activity prevents the synaptic dysfunction driven by otau in the Schaffer collateral synapses in the WT mouse hippocampus. fEPSPs were evaluated following standard HFS protocol (3 × 100 Hz) depicted by three arrows in (B) and (C) and compared to the baseline and plotted as a percentage of the original value (A–C). Application of the oligomers follows the schematic depicted in the gray box above the graphs. Representative traces are provided next to the bars or symbols, with the length of the vertical scale bar at 0.5 mV and the horizontal scale bar at 10 ms. The application of the inhibitor was started 15 minutes before the application of the oligomers and continued through the time that the slices were incubated with the oligomers. (A) As the otau concentration increased from 5 nM to 500 nM, the HFS LTP (last 10 minutes) decreased from ∼275% to ∼100% (clear bars—5 nM otau: 270.90 ± 8.401, n = 6; 50 nM otau: 156.00 ± 5.892, n = 12; and 500 nM otau: 98.52 ± 5.425, n = 6). Both the PLD1-specific inhibitor (VU0155069, filled squares) and PLD2-specific inhibitor (VU0364739, filled triangles) were ineffective in suppressing the LTP effect of 50 nM otau at the lowest concentration tested (2 nM PLD1 inhibitor: 161.7 ± 4.035, n = 6 and 2 nM PLD2 inhibitor: 157.4 ± 4.780, n = 6). However, whereas the PLD1 inhibitor at higher concentrations (20 nM: 302.5 ± 6.775, n = 6 and 200 nM: 302.0 ± 5.349, n = 6) was effective in suppressing the otau-driven HFS-LTP deficits, PLD2 inhibitor was ineffective in attenuating or reducing the otau effects on HFS LTP (20 nM – 158.7 ± 5.196, n = 6 and 200 nM – 158.5 ± 5.768, n = 6). (B) PLD1 inhibitor at 20 nM (inverted hollow triangles) and 200 nM (filled circles) shows complete recovery of the Schaffer collateral HFS LTP including PTP (first 10 minutes) and LTP (last 10 minutes), whereas the inhibitor at 2 nM (hollow hexagons) is ineffective in overcoming the effect of otau inhibition (50 nM, hollow squares). (C) The PLD2 inhibitor is ineffective at all concentrations (2 nM: hollow hexagons, 20 nM: hollow squares, and 200 nM: filled circles) against the LTP deficits seen with otau (50 nM: hollow squares). Statistical significance was assessed using nonparametric one-way ANOVA (Kruskal-Wallis test) followed by Dunn's multiple comparison. Abbreviations: Aβ, amyloid β; ANOVA, analysis of variance; fEPSP, field excitatory postsynaptic potential; PLD, phospholipase D; PLD1, phospholipase D isoform 1; PLD2, phospholipase D isoform 2; oAβ, oligomeric Aβ; HFS, high-frequency stimulation; LTP, long-term potentiation; otau, oligomeric tau species; PTP, posttetanic potentiation; WT, wild-type.

change from the initial average baseline fEPSP slope, which was defined as the average slope obtained for 10 minutes before HFS.

2.8. Novel object recognition behavior

Experiments were performed as described previously [29]. The time spent exploring each object was recorded using ObjectScan (Clever Sys, Inc.); an area of 2 cm^2 surrounding the object is defined such that nose entries within 2 cm of the object were recorded as time exploring the object. After a retention interval of 2–24 hours, novel object memory was tested. The animal was allowed 10 minutes, during which the amount of time exploring each object was recorded. Oligomers (generated as per Section 2.6) were administered intracerebroventricularly using standard procedures [30] either 2 hours before training (oAβ) or 2 hours before habituation day 2 (otau). The PLD1 inhibitor was administered intraperitoneally 15 minutes before the training phase. Objects were randomized and counterbalanced across animals. For novel object recognition (NOR) tests, the percent time exploring each object (familiar versus novel) is reported as an object discrimination index [29].

2.9. Statistics

To account for non-normal distribution of data, either nonparametric *t*-tests (Mann-Whitney *U* or Wilcoxon rank sum) or one-way analyses of variance (Kruskal-Wallis test) followed by Dunn's multiple comparison when significance was achieved were used. Statistical significance was defined as $P < .05$. Power analyses indicate that approximately six animals per group (including losses commonly occurring in long-term studies) will give reasonable variances for the behavioral analyses, electrophysiological studies, and biochemical correlates. Sample size was based on calculations using G*Power software assuming an effect size of 0.85 and a power of 0.8 with an α error probability of 0.05. A minimum of three males and three females was studied, and if there were no sex differences, the data were pooled.

3. Results

3.1. Synaptosomal PLD1/PLD2 levels are differentially altered in brains from postmortem AD patients compared to age-matched controls

Synaptosomal fractions from the frontal cortex, temporal cortex, and hippocampal tissues (see Table 1 for details of the patient samples used) were assessed for PLD1 and PLD2 expression (Fig. 4). AD hippocampal (Fig. 4A) PLD1 expression was increased (~50%) compared to controls. Likewise, AD temporal cortex PLD1 levels (Fig. 4C) were significantly increased compared to controls. However, AD frontal cortex PLD1 levels (Fig. 4E) were significantly lowered (~50%) compared to controls.

PLD2 levels in the hippocampus (Fig. 4B) and temporal cortex (Fig. 4D) of the AD group were not significantly different, whereas the frontal cortex (Fig. 4F) expressed low levels of PLD2 [similar to PLD1 (Fig. 4E)]. These results provide the first evidence that synaptic PLD1, not PLD2, levels are elevated in the human brain regions of the temporal cortex and hippocampus, which are documented to show severe effects of degeneration [31].

3.2. Increased PLD1 expression observed in response to oAβ acute application in mouse brain slices

We assessed the early events of AD-like synapse dysfunction/memory using our well-established biochemical, behavioral, and electrophysiological studies in our laboratory [27]. We observed a marked enhancement in the phosphorylation at threonine 147 of PLD1 in the oAβ-incubated slices compared to controls (Fig. 4A). In addition, we also observed that a small-molecule PLD1 inhibitor (VU0155069, 20 nM—validated in our previous study [13]), applied 15 minutes before application of oAβ (Fig. 1A), prevents the activation of PLD1. Moreover, even synaptosomal PLD1 was significantly increased following incubation with oAβ where PLD1 inhibitor application prevented the increase (Fig. 1B). Cytoplasmic expression of PLD1 was not altered (data not shown).

3.3. Age-dependent elevation of hippocampal PLD1 observed in 3XTg-AD mice

In the 3XTg-AD transgenic mouse model, accumulation of Aβ and earliest memory deficits were reported at 6 months of age, whereas elevation of both Aβ and tau was reported at 12 months of age [32]. We observe (Fig. 1C) a progressive increase in PLD1 expression from 6 to 12 to 18 months of age.

3.4. Inhibiting PLD isoforms prevent oAβ-driven HFS-LTP deficits in the mouse hippocampus

After establishing concentration-dependent HFS long-term potentiation (LTP) decrease with oAβ application (Fig. 2A), we used 200 nM of oAβ as the optimal concentration to address whether inhibiting PLD function prevents oAβ-driven HFS-LTP deficit. Both PLD1- (Fig. 1A and 1B) and PLD2-specific inhibitors (Fig. 1A and 1C) were ineffective in suppressing the LTP effect of 200 nM oAβ at the lowest concentration of inhibitors (2 nM) tested but prevented the oAβ-driven LTP deficit at higher concentrations (20 and 200 nM).

3.5. Inhibiting PLD1, but not PLD2, prevents otau-driven HFS-LTP deficit in the mouse hippocampus

Using an optimal concentration of otau (50 nM, Fig. 3A) that partially inhibits the HFS LTP in wild-type mouse hippocampi, we observed that 20 nM or 200 nM of the

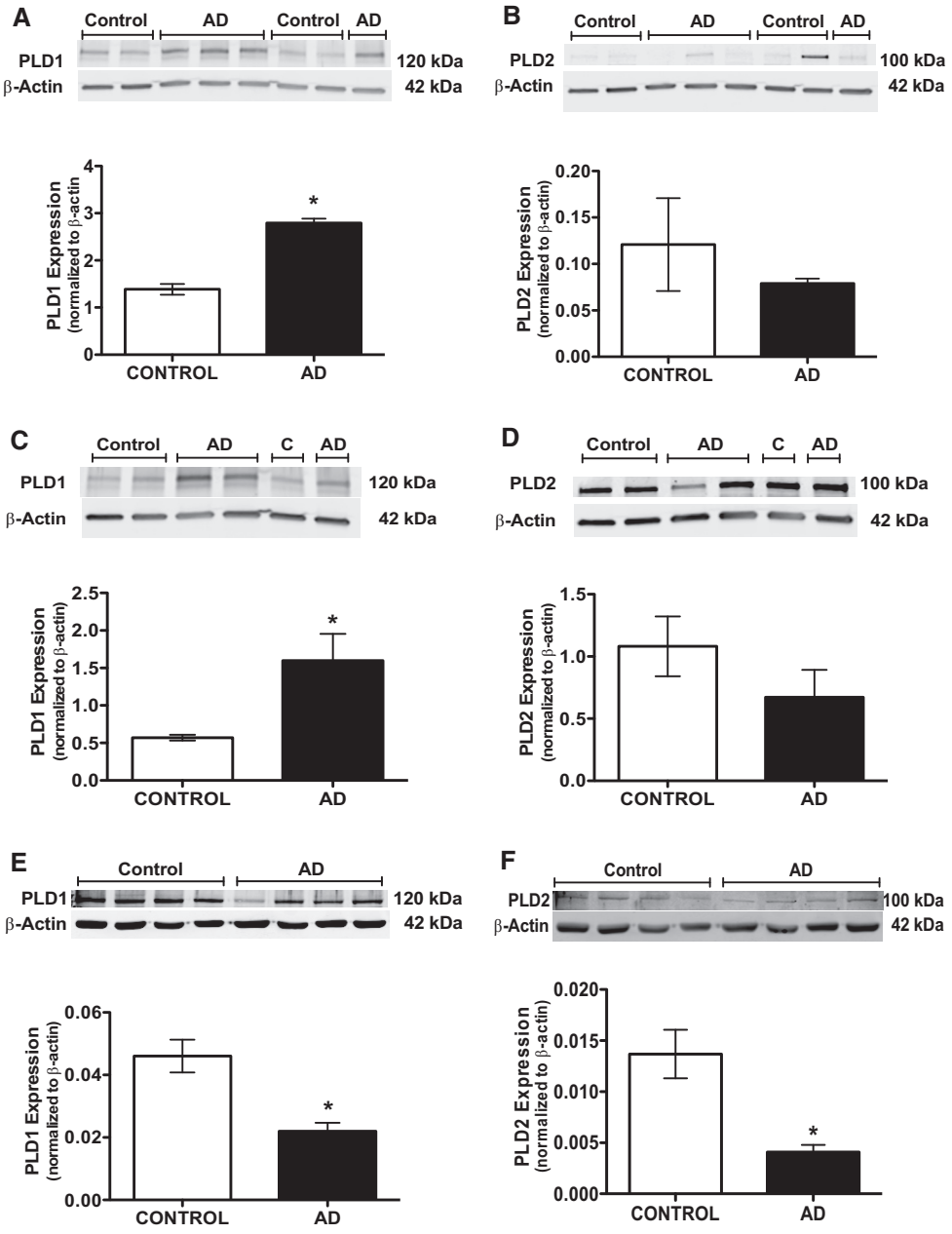

Fig. 4. Synaptosomal expression of PLD1 (A, C), not PLD2 (B, D), is increased in the hippocampal and temporal cortex in AD patients (black bars) compared to age-matched controls (hollow bars). After the synaptosomes were prepared from the appropriate brain regions of the hippocampus (A, B), temporal cortex (C, D), and frontal cortex (E, F), the samples were coded and provided to the experimenter to perform the Western blots, resulting in the patterns of loading seen in each panel. (A) Hippocampal PLD1 expression of the AD group (2.791 ± 0.093, n = 4) was increased ∼50% (*$P < .05$) compared to controls (1.387 ± 0.115, n = 4). Likewise, (C) AD temporal cortex PLD1 levels (1.597 ± 0.358, n = 3) were significantly increased (*$P < .05$) compared to controls (0.571 ± 0.038, n = 3). Interestingly, (E) AD frontal cortex PLD1 levels (0.022 ± 0.003, n = 4) were significantly lowered ∼50% (*$P < .05$) compared to controls (0.046 ± 0.005, n = 4). In contrast, PLD2 levels in the (B) hippocampus (AD: 0.079 ± 0.005, n = 4, vs. control: 0.136 ± 0.120, n = 4; $P = .34$) and (D) temporal cortex (AD: 0.672 ± 0.219, n = 3, vs. control: 1.081 ± 0.241, n = 3; $P = .21$) were not significantly different, whereas the (F) frontal cortex (AD: 0.004 ± 0.001, n = 4, vs. control: 0.014 ± 0.002, n = 4; *$P < .05$) expressed low levels similar to frontal cortex PLD1 expression. Each lane in the blots above the graph represents the protein sample from one human subject brain area. A total of 11 AD and 8 control brain regions were used (details provided in Table 1). * indicates $P < .05$ compared to controls. Statistical significance was assessed using nonparametric analysis to account for the sample size and distribution using Mann-Whitney *U* post hoc analysis. Abbreviations: AD, Alzheimer's disease; PLD1, phospholipase D isoform 1; PLD2, phospholipase D isoform 2.

PLD1 inhibitor (VU0155069) was sufficient in blocking the effects of otau. Interestingly, 2 nM of the PLD1 inhibitor and all concentrations of the PLD2 inhibitor (VU0364739) did not prevent the otau-dependent inhibition of HFS LTP (Fig. 3A and 3C), suggesting that PLD2 activation is not recruited in otau-driven HFS-LTP deficits.

Thus, based on the aforementioned collective results, we further investigated the effects of PLD1 isoform–specific inhibition on AD-like synaptic dysfunction and underlying memory deficits.

3.6. PLD1 inhibition attenuates HFS-LTP deficits in the 3XTg-AD mice

We used 3XTg-AD mice (that show progressive elevation of PLD1 expression in Western blots [Fig. 1C]) to further assess PLD1 inhibition in preventing synergistic effects of oAβ or otau corresponding to decreased HFS LTP attributed to Aβ (at 6 months) and then both Aβ and tau (12 months onward).

After an acute injection of the PLD1 inhibitor (10 mg/kg intraperitoneal) or vehicle (0.9% saline solution, 1 mg/mL) at two different ages, 6 months (Fig. 5A and 5C) and 18 months (Fig. 5B and 5C), animals were sacrificed after 24 hours to study hippocampal HFS LTP. We used 3XTg-AD females because the effects of the transgenes were reported to be less severe in the males [33]. Compared to the age-matched controls, HFS LTP was markedly reduced in the vehicle-treated 3XTg-AD mice. Interestingly, HFS-LTP deficits were not only prevented but also restored in PLD1 inhibitor–injected mice compared to levels observed in healthy age-matched control mice.

3.7. PLD1 inhibition rescues oAβ- or otau-driven NOR memory deficits

We used the NOR paradigm that our group uses routinely to assess hippocampal-dependent memory deficits [29]. The PLD1 inhibitor (10 mg/kg intraperitoneal) blocked oAβ-mediated (3 μL of a 95 μM intracerebroventricular) NOR deficits of short-term (2 hours, Fig. 6A) and long-term memory (24 hours, Fig. 6B). We, further, assessed and observed that PLD1 inhibition is also effective in preventing otau-mediated memory deficits in the short-term (2 hours, Fig. 6C) and long-term (24 hours, Fig. 6D). None of the groups showed any detriments in their locomotor behavior or exploration time (data not shown).

4. Discussion

4.1. Main findings

The main findings of the present study are the following: (1) PLD1, the inducible isoform of phosphatidylcholine cleaving PLD, is elevated in the synaptosomes from AD patients' hippocampus and temporal cortex compared to age-matched controls; (2) Interestingly, PLD2, the constitutive isoform, is not changed in synaptosomal expression in the AD hippocampus or the temporal cortex but shows marked reduction in the frontal cortex (similar to PLD1) compared to age-matched controls; (3) Hippocampal synaptosomal expression of PLD1 and its activated form (phosphorylated at T147) was increased by acute administration of oAβ; (4) Hippocampal synaptosomal expression of PLD1 also showed an age-dependent increase in AD-like memory deficits modeled in 3XTg-AD mice, where the progression of Aβ plaques and tau tangles follows a timeline of expression paralleling the human neuropathology; (5) Specific inhibition of PLD1 or PLD2 isoform in hippocampal brain slices from C57Bl/6 mice is sufficient to prevent the oAβ-driven synaptic dysfunction (HFS LTP) at the Schaffer collateral synapses; (6) Interestingly, only PLD1-specific inhibition was effective in blocking the otau-driven HFS-LTP deficits; (7) PLD1-specific inhibition was sufficient to prevent the hippocampal HFS-LTP deficits driven by transgenic overexpression of human Aβ and tau in the 3XTg-AD mice at 6 months (earlier stages) and 18 months (later stages) of the AD-like memory deficit progression; and (8) PLD1-specific inhibition was effective in preventing the NOR deficits induced by either oAβ or otau in C57Bl/6 male and female mice.

4.2. Differential PLD expression patterns in postmortem human brain regions affected in AD

It was demonstrated that PLD1 expression was increased in the neurons in mouse hippocampal mossy fiber sprouting, whereas PLD2-increased expression occurred in the astrocytes, suggesting that neuronal PLD1, linked to regulation of secretion and secretory granule exocytosis, is important for modulating neuronal plasticity by directly affecting synaptic neurotransmission [34]. On the other hand, recent studies where PLD1 levels are completely lowered in PLD1 knockout mice noted only a minor delay in brain development, with a limited impairment in cognitive function [35]. Thus, one can speculate that neuropathology of lower levels of PLD1 and PLD2 in the AD frontal cortex are of less concern than the elevated levels of PLD1 in the AD hippocampus/temporal cortex. However, such a correlative speculation is a limitation that needs further investigation, which is beyond the scope of the present study. More importantly, elevated PLD1 is of greater concern because it is also observed in neoplastic disorders (along with elevated PLD2) and is the active subject of small-molecule inhibitor development toward therapeutics [8]. Thus, increased PLD activity reported in postmortem AD brains [14] may be a result of PLD1 overexpression, and we, therefore, addressed whether PLD1 is involved with the synaptic dysfunction and underlying memory deficits associated with AD.

4.3. oAβ can activate neuronal PLD1 expression

Previous studies proposed a neuroprotective role for PLD1 where a direct effect of overexpressed PLD1 on presenilin-1 results in reduction of Aβ species generation [16], by promoting trans-Golgi intracellular trafficking of β APP and promoting neurite outgrowth [17]. Perhaps, the elevated PLD1 levels in the activated astrocytes and mitochondrial fractions of AD brains, reported in another set of

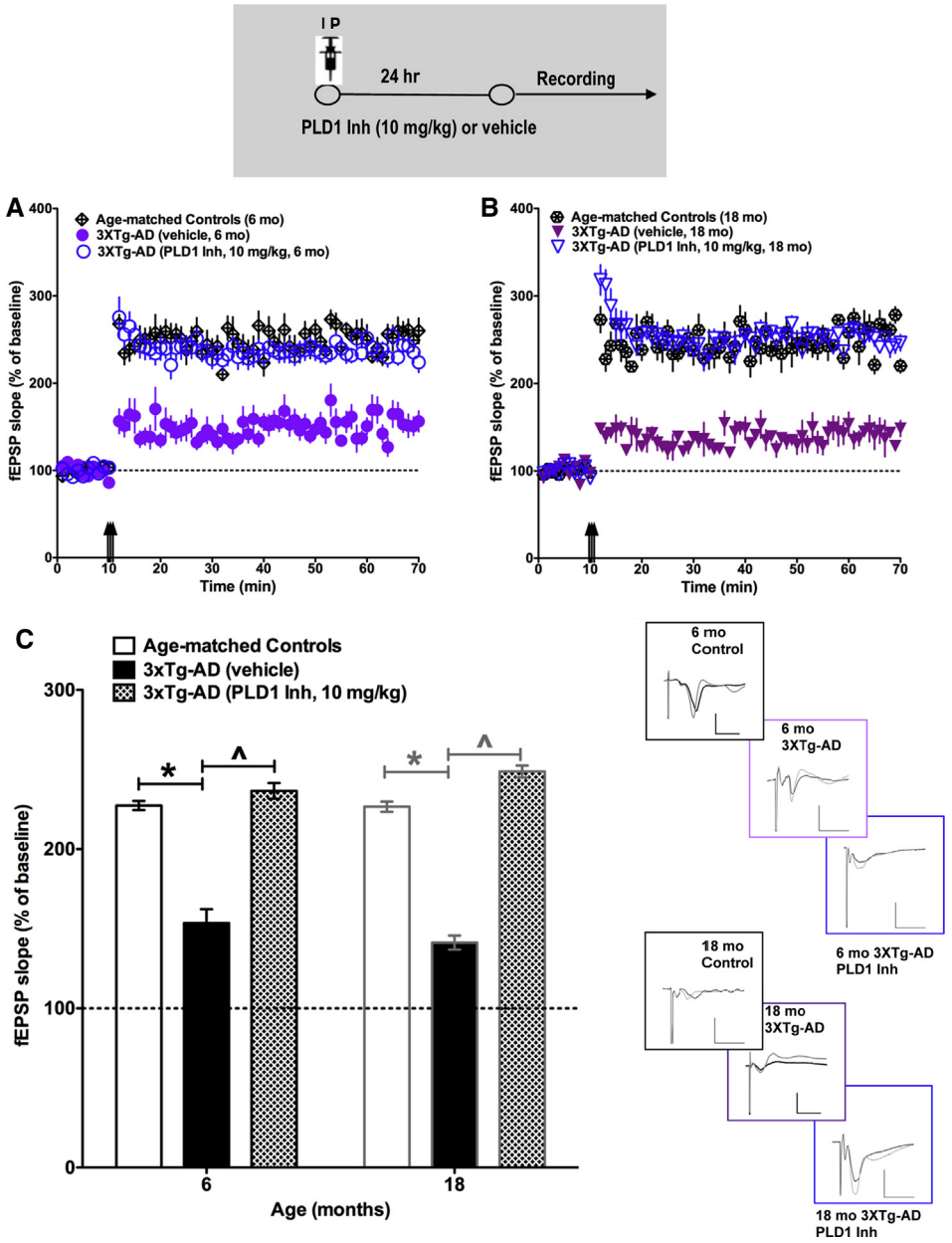

Fig. 5. Acute inhibition of PLD1 isoform activity is sufficient to prevent synaptic dysfunction driven by amyloidogenic proteins at 6 months and at 18 months in the 3XTg-AD mouse model. fEPSPs were evaluated following standard HFS protocol (3 × 100 Hz) depicted by three arrows in (A) and (B) and compared to the baseline and plotted as a percentage of the original value. Representative traces are provided next to the bars or symbols, with the length of the vertical scale bar at 0.5 mV and the horizontal scale bar at 10 ms. The effect of the PLD1 inhibitor was assessed using intraperitoneal injection of 10-mg/kg PLD1 inhibitor (VU0155069) into the mouse or vehicle (0.9% saline, 1 mL/kg), and the animal returned to its cage 24 hours before the electrophysiological analysis (see the gray box above the graphs). Synaptic dysfunction, occurring due to progressive accumulation of Aβ (6 months) or Aβ and tau (18 months), were assessed. (A) At 6 months of age, the age-matched control group shows potentiation (∼220%) following HFS protocol (crossed diamonds), whereas the vehicle-treated 3XTg-AD group (filled circles) has a significantly reduced (∼140%) potentiation. Administration of the PLD1 inhibitor blocked the synaptic dysfunction in the 3XTg-AD mice and restored the potentiation following HFS (∼250%, hollow circles). (B) At 18 months of age, the LTP (∼220%, crossed hexagons) observed in age-matched controls was diminished in the 3XTg-AD mice (∼130%, filled inverted triangles), and once again, acute administration of the PLD1 inhibitor was sufficient to restore the potentiation (∼230%, hollow inverted triangles) in the 3XTg-AD mice. (C) When assessed at early (6 months) or late stages (18 months) of AD-like memory deficit progression, LTP (measured at the last 10 minutes of the post-HFS recording) is significantly reduced in the 3XTg-AD mice treated with vehicle (filled bars—6 months: 142.6 ± 2.471, n = 9 and 18 months: 132.5 ± 1.916, n = 5) compared to age-matched controls (hollow bars—6 months: 227.4 ± 6.341, n = 4 and 18 months: 226.7 ± 6.432, n = 5) and compared to the PLD1 inhibitor–treated 3XTg-AD mice (hatched bars—6 months: 236.6 ± 8.626, n = 9 and 18 months: 248.8 ± 6.460, n = 5). Statistical significance was assessed using nonparametric one-way ANOVA (Kruskal-Wallis test) followed by Dunn's multiple comparison test. * indicates $P < .05$ compared to the control group, whereas ^ indicates $P < .05$ compared to the PLD1 inhibitor application group. Abbreviations: 3XTg-AD, mouse model with overexpression of human amyloid precursor protein, presenilin-1 gene, and microtubule-associated protein tau; AD, Alzheimer's disease; ANOVA, analysis of variance; fEPSP, field excitatory postsynaptic potential; IP, intraperitoneal; PLD1, phospholipase D isoform 1; HFS, high-frequency stimulation; LTP, long-term potentiation.

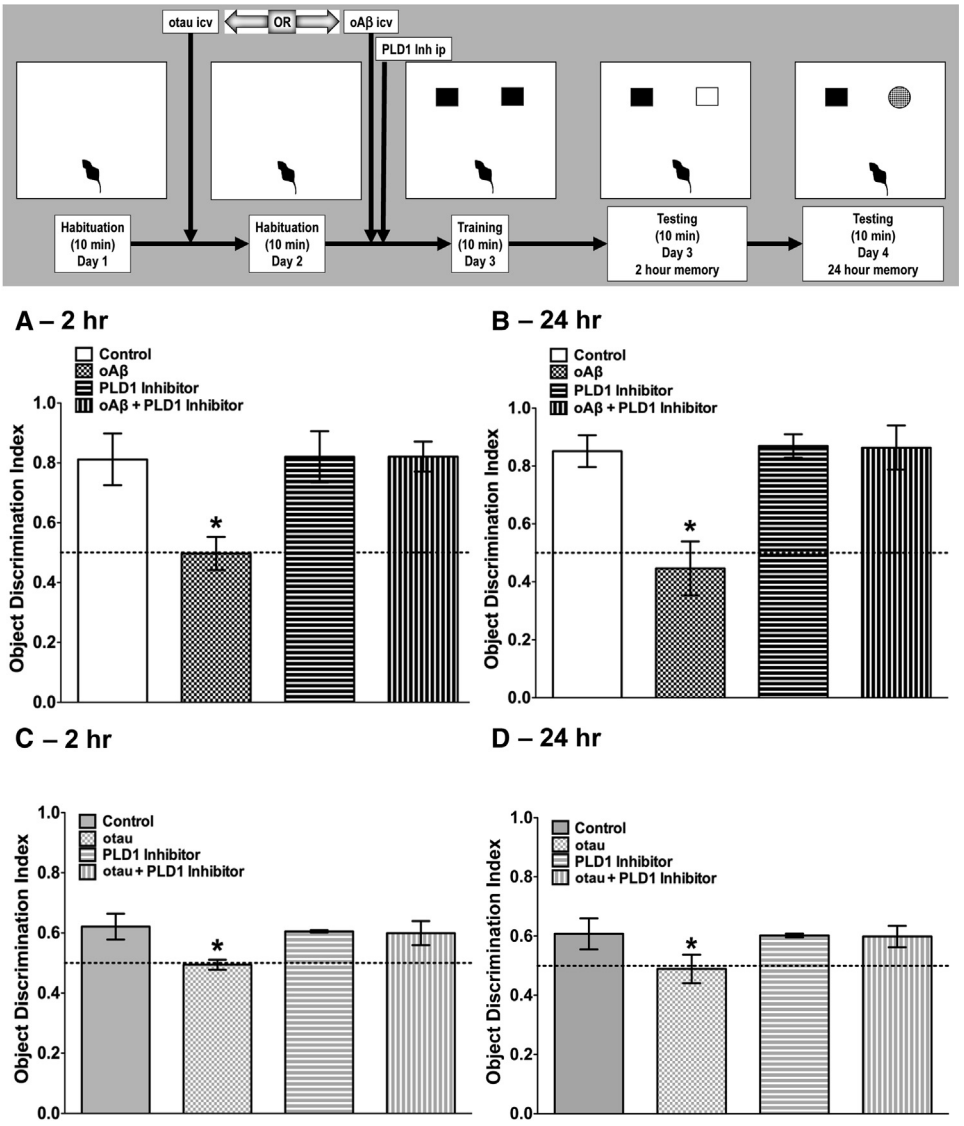

Fig. 6. The PLD1 inhibitor injected ip following oAβ (A, B) or otau (C, D) icv prevents the respective oligomer-induced memory deficits. Male and female C57Bl/6 mice were habituated, trained, and tested as shown in the gray panel. NOR memory for 2 hours (A, C) and 24 hours (B, D) was tested using (A and B) either vehicle (0.9% saline, 1 mg/mL ip) or PLD1 inhibitor (VU0155069, 10 mg/kg ip) injected 2 hours after oAβ (3 μL of a 95-μM stock icv) or vehicle (ACSF, 3 μL icv) and (C and D) either vehicle (0.9% saline, 1 mg/mL ip) or PLD1 inhibitor (VU0155069, 10 mg/kg ip) injected 24 hours after otau (3 μL of a 1-μM stock icv) or vehicle (ACSF, 3 μL icv). (A) After 2 hours of training, animals injected with saline and given ACSF icv (white bar, 0.811 ± 0.087, n = 6) spent more time with the novel object, compared to the older object, whereas the animals treated with oAβ (cross-hatched bar: 0.497 ± 0.0551, n = 6) showed no discrimination between the two objects. While the PLD1 inhibitor–treated animals (horizontal bars, 0.820 ± 0.086, n = 6) showed no deficits, the PLD1 inhibitor treatment before oAβ icv (vertical bars, 0.821 ± 0.051, n = 6) was effective in preventing the memory deficit mediated by oAβ. (B) The same group of animals were tested 24 hours after their training session, using a new (round) novel object—the control group of animals still showed increased time in the novel object zone (vehicle + saline: 0.852 ± 0.055, n = 6), while the oAβ group showed no discrimination between the new and the old object (oAβ + saline: 0.446 ± 0.093, n = 6). There was no difference in the NOR memory at 24 hours following PLD1 inhibitor treatment with (oAβ + PLD1 inhibitor: 0.864 ± 0.076, n = 6) or without oAβ (vehicle + PLD1 inhibitor: 0.870 ± 0.041, n = 6). (C) After 2 hours of training, animals injected with saline and given ACSF icv (gray bar, 0.621 ± 0.0432, n = 6) spent more time with the novel object, compared to the older object, whereas the animals treated with otau (cross-hatched bar: 0.494 ± 0.016, n = 6) showed no discrimination between the two objects. Again, PLD1 inhibitor treatment, by itself, did not affect NOR (horizontal bars: 0.605 ± 0.004, n = 6) but was effective in preventing otau-mediated NOR deficits (vertical bars: 0.600 ± 0.040, n = 6). (D) After 24 hours to their training session, the control group of animals still spent more time in the novel object zone (vehicle + saline: 0.607 ± 0.052, n = 6), whereas the otau group showed no discrimination between the new and the old object (otau + saline: 0.489 ± 0.048, n = 6). Once again, PLD1 inhibitor treatment was effective after 24 hours in preventing the otau-driven memory deficits (otau + PLD1 inhibitor: 0.598 ± 0.036, n = 6) while having no detrimental effect when applied without any otau (vehicle + PLD1 inhibitor: 0.602 ± 0.006, n = 6). For each data point, n = 6 animals (3 males and 3 females), and there were no sex differences observed. Statistical significance was assessed using nonparametric one-way ANOVA (Kruskal-Wallis test) followed by Dunn's multiple comparison test. * indicates $P < .05$ compared to control/PLD1 Inhibitor treated/oligomer + PLD1 Inhibitor treated. Abbreviations: Aβ, amyloid β; ANOVA, analysis of variance; ACSF, artificial cerebrospinal fluid; icv, intracerebroventricularly; ip, intraperitoneal; NOR, novel object recognition; oAβ, oligomeric Aβ; otau, oligomeric tau species; PLD1, phospholipase D isoform 1.

studies [18,36], could be explained as neuroprotective. However, the authors indicate that the amyloid region of APP interacts with PLD1 and increased APP expression stimulates PLD1 activity, thus questioning the speculated neuroprotective role of PLD1. Although PLD2 studies were conducted in transgenic mouse models to demonstrate a direct role in Aβ pathology [15], such functional studies for the role of PLD1 in AD-like memory deficits in mouse models are lacking. As a result, we first demonstrate that oAβ acute application, indeed, activates PLD1 expression in mouse hippocampal slices. This is in agreement with the earlier studies that used activated astrocytes and mitochondrial fractions of AD brains [18,36]. We, further, show that hippocampal synaptosomal PLD1 levels increase as a function of age in transgenic mice documented to show progressive upregulation of human Aβ and tau. Collectively, these results definitively demonstrate that neuronal PLD1 levels can be upregulated by amyloidogenic proteins (that are important for AD-like memory deficits) and therefore question the neuroprotective role of PLD1.

4.4. Hippocampal CA3-CA1 synaptic dysfunction or NOR memory deficits driven by oAβ or otau can be blocked by preventing PLD1-specific activity

The parent compound from which the PLD1-specific inhibitor was developed [8] is well tolerated in humans. Thus, targeting the inducible PLD1 isoform holds great promise in being developed rapidly as an intervention in preventing AD-like cognitive decline. Our systematic assessment demonstrates a definitive role for PLD1 in mediating AD-like memory deficits. We also observed that PLD1 inhibition blocks the combined early-stage (Aβ driven) and late-stage (Aβ and tau driven) synaptic dysfunction in the 3XTg-AD mouse hippocampus [19,37]. A crucial role for rapid action of PLD1 activity was first described in *Aplysia* [38], where altering the phospholipid-dependent fusogenic status of neurotransmitter vesicles at the presynaptic release sites can affect synaptic homeostasis [39] leading to Aβ neurotoxicity–driven synaptic hypoactivity [40] as an immediate change. Prolonged increase in PLD1 levels can result in both negative (RhoA-PLD1-phosphatidic acid mediated) regulation of dendritic branching [41] and positive (inhibiting ADAM10-driven N-cadherin cleavage mediated) regulation of [42] dendritic spine development. Both reduction of ADAM10 [43] and upregulation of RhoA signaling [44] are known to occur in AD-like memory deficits. Based on these observations, we speculate that the immediate effects of PLD1 on HFS LTP may occur via Aβ neurotoxicity–driven synaptic hypoactivity reported earlier [40]. However, further studies are required to elucidate how prolonged elevated PLD1 signaling affects signaling partners such as RhoA, PKCα [45], mTOR [46], cofilin, [47] and depolymerized F-actin [48], in contributing toward AD-like synaptic dysfunction and underlying memory deficits.

Nevertheless, targeting the inducible PLD1 isoform holds great promise in being developed rapidly as an intervention in preventing AD-like cognitive decline, thus complementing existing approaches studying immunogenic suppression of oAβ and otau toward stopping the progression of AD.

Acknowledgments

This work was supported by the National Institutes of Health (grant number NIH 1R01AG042890), Alzheimer's Association Research Grant (AARG-17-533363) to B.K., and the Mitchell Center for Neurodegenerative Diseases. The authors would like to thank Randy Woltjer, MD, PhD, at the Oregon Health and Science University Layton Aging and Alzheimer's Center for providing the human samples used in the present study. The authors would also like to acknowledge Anusha Srinivasan for critically reading and editing the manuscript.

RESEARCH IN CONTEXT

1. Systematic review: In studying the role of phospholipase D signaling in memory, the corresponding author has surveyed the literature using traditional resources, international conferences, and meeting abstracts. The citations of previous studies on proposed mechanism of phospholipase D in memory and Alzheimer's disease pathology are included in the present study.
2. Interpretation: Earlier studies predicted a protective role for phospholipase D isoform 1 (PLD1) in amyloid precursor protein trafficking while implicating phospholipase D isoform 2 in assisting amyloid β–driven synaptic dysfunction and memory deficits. However, our present study demonstrates that PLD1 overexpression in Alzheimer's disease brains contributes to the synaptic dysfunction and underlying memory deficits driven by amyloidogenic proteins.
3. Future directions: The present systematic study in humans and transgenic mouse models proposes the need for additional investigation into (1) how PLD1 overexpression in specific brain regions are detrimental to synaptic strengthening and (2) explore therapeutic potential of PLD1 inhibition in preventing/stopping progression of Alzheimer's disease–related memory deficits.

References

[1] 2017 Alzheimer's disease facts and figures. Alzheimers Dement 2017; 13:325–73.

[2] Selkoe DJ, Hardy J. The amyloid hypothesis of Alzheimer's disease at 25 years. EMBO Mol Med 2016;8:595–608.

[3] Iqbal K, Liu F, Gong CX. Tau and neurodegenerative disease: the story so far. Nat Rev Neurol 2016;12:15–27.

[4] Rosenblum WI. Why Alzheimer trials fail: removing soluble oligomeric beta amyloid is essential, inconsistent, and difficult. Neurobiol Aging 2014;35:969–74.

[5] Panza F, Solfrizzi V, Seripa D, Imbimbo BP, Lozupone M, Santamato A, et al. Tau-centric targets and drugs in clinical development for the treatment of Alzheimer's disease. Biomed Res Int 2016;2016:3245935.

[6] Arendt T. Synaptic degeneration in Alzheimer's disease. Acta Neuropathol 2009;118:167–79.

[7] Wirz KT, Keitel S, Swaab DF, Verhaagen J, Bossers K. Early molecular changes in Alzheimer disease: can we catch the disease in its presymptomatic phase? J Alzheimers Dis 2014;38:719–40.

[8] Brown HA, Thomas PG, Lindsley CW. Targeting phospholipase D in cancer, infection and neurodegenerative disorders. Nat Rev Drug Discov 2017;16:351–67.

[9] Nelson RK, Frohman MA. Physiological and pathophysiological roles for phospholipase D. J Lipid Res 2015;56:2229–37.

[10] Frohman MA. The phospholipase D superfamily as therapeutic targets. Trends Pharmacol Sci 2015;36:137–44.

[11] Krishnan B, Scott MT, Pollandt S, Schroeder B, Kurosky A, Shinnick-Gallagher P. Fear potentiated startle increases phospholipase D (PLD) expression/activity and PLD-linked metabotropic glutamate receptor mediated post-tetanic potentiation in rat amygdala. Neurobiol Learn Mem 2016;128:65–79.

[12] Krishnan B, Genzer KM, Pollandt SW, Liu J, Gallagher JP, Shinnick-Gallagher P. Dopamine-induced plasticity, phospholipase D (PLD) activity and cocaine-cue behavior depend on PLD-linked metabotropic glutamate receptors in amygdala. PLoS One 2011;6:e25639.

[13] Krishnan B. Amygdala-hippocampal Phospholipase D (PLD) signaling as novel mechanism of cocaine-environment maladaptive conditioned responses. Int J Neuropsychopharmacol 2016;19:pyv139.

[14] Kanfer JN, Singh IN, Pettegrew JW, McCartney DG, Sorrentino G. Phospholipid metabolism in Alzheimer's Disease and in a human cholinergic cell. J Lipid Mediat Cell Signal 1996;14:361–3.

[15] Oliveira TG, Chan RB, Tian H, Laredo M, Shui G, Staniszewski A, et al. Phospholipase d2 ablation ameliorates Alzheimer's disease-linked synaptic dysfunction and cognitive deficits. J Neurosci 2010; 30:16419–28.

[16] Cai D, Netzer WJ, Zhong M, Lin Y, Du G, Frohman M, et al. Presenilin-1 uses phospholipase D1 as a negative regulator of beta-amyloid formation. Proc Natl Acad Sci U S A 2006;103:1941–6.

[17] Cai D, Zhong M, Wang R, Netzer WJ, Shields D, Zheng H, et al. Phospholipase D1 corrects impaired APP trafficking and neurite outgrowth in familial Alzheimer's disease-linked presenilin-1 mutant neurons. Proc Natl Acad Sci U S A 2006;103:1936–40.

[18] Jin JK, Ahn BH, Na YJ, Kim JI, Kim YS, Choi EK, et al. Phospholipase D1 is associated with amyloid precursor protein in Alzheimer's disease. Neurobiol Aging 2007;28:1015–27.

[19] Oddo S, Caccamo A, Shepherd JD, Murphy MP, Golde TE, Kayed R, et al. Triple-transgenic model of Alzheimer's disease with plaques and tangles: intracellular Abeta and synaptic dysfunction. Neuron 2003; 39:409–21.

[20] Braak H, Braak E. Neuropathological stageing of Alzheimer-related changes. Acta Neuropathol 1991;82:239–59.

[21] Braak H, Braak E. Morphological criteria for the recognition of Alzheimer's disease and the distribution pattern of cortical changes related to this disorder. Neurobiol Aging 1994;15:355–6. discussion 379–380.

[22] Franklin W, Taglialatela G. A method to determine insulin responsiveness in synaptosomes isolated from frozen brain tissue. J Neurosci Methods 2016;261:128–34.

[23] Garber JC. Guide for the Care and Use of Laboratory Animals. C.f.t.U.o.t.G.f.t.C.a.U.o.L.A.N.R. Council. Washington (DC): The National Academies Press; 2011.

[24] Dineley KT, Kayed R, Neugebauer V, Fu Y, Zhang W, Reese LC, et al. Amyloid-beta oligomers impair fear conditioned memory in a calcineurin-dependent fashion in mice. J Neurosci Res 2010; 88:2923–32.

[25] Gerson JE, Sengupta U, Kayed R. Tau oligomers as pathogenic seeds: preparation and propagation in vitro and in vivo. Methods Mol Biol 2017;1523:141–57.

[26] Ting JT, Daigle TL, Chen Q, Feng G. Acute brain slice methods for adult and aging animals: application of targeted patch clamp analysis and optogenetics. Methods Mol Biol 2014;1183:221–42.

[27] Comerota MM, Krishnan B, Taglialatela G. Near infrared light decreases synaptic vulnerability to amyloid beta oligomers. Sci Rep 2017;7:15012.

[28] Martin ZS, Neugebauer V, Dineley KT, Kayed R, Zhang W, Reese LC, et al. alpha-Synuclein oligomers oppose long-term potentiation and impair memory through a calcineurin-dependent mechanism: relevance to human synucleopathic diseases. J Neurochem 2012; 120:440–52.

[29] Taglialatela G, Hogan D, Zhang WR, Dineley KT. Intermediate- and long-term recognition memory deficits in Tg2576 mice are reversed with acute calcineurin inhibition. Behav Brain Res 2009;200:95–9.

[30] Clark WG, Vivonia CA, Baxter CF. Accurate freehand injection into the lateral brain ventricle of the conscious mouse. J Appl Physiol 1968;25:319–21.

[31] Braak H, Del Tredici K. The preclinical phase of the pathological process underlying sporadic Alzheimer's disease. Brain 2015; 138:2814–33.

[32] Stover KR, Campbell MA, Van Winssen CM, Brown RE. Early detection of cognitive deficits in the 3xTg-AD mouse model of Alzheimer's disease. Behav Brain Res 2015;289:29–38.

[33] Clinton LK, Billings LM, Green KN, Caccamo A, Ngo J, Oddo S, et al. Age-dependent sexual dimorphism in cognition and stress response in the 3xTg-AD mice. Neurobiol Dis 2007;28:76–82.

[34] Klein J. Functions and pathophysiological roles of phospholipase D in the brain. J Neurochem 2005;94:1473–87.

[35] Burkhardt U, Stegner D, Hattingen E, Beyer S, Nieswandt B, Klein J. Impaired brain development and reduced cognitive function in phospholipase D-deficient mice. Neurosci Lett 2014;572:48–52.

[36] Jin JK, Kim NH, Lee YJ, Kim YS, Choi EK, Kozlowski PB, et al. Phospholipase D1 is up-regulated in the mitochondrial fraction from the brains of Alzheimer's disease patients. Neurosci Lett 2006; 407:263–7.

[37] Fa M, Puzzo D, Piacentini R, Staniszewski A, Zhang H, Baltrons MA, et al. Extracellular tau oligomers produce an immediate impairment of LTP and memory. Sci Rep 2016;6:19393.

[38] Humeau Y, Vitale N, Chasserot-Golaz S, Dupont JL, Du G, Frohman MA, et al. A role for phospholipase D1 in neurotransmitter release. Proc Natl Acad Sci U S A 2001;98:15300–5.

[39] Small DH. Mechanisms of synaptic homeostasis in Alzheimer's disease. Curr Alzheimer Res 2004;1:27–32.

[40] Small DH. Network dysfunction in Alzheimer's disease: does synaptic scaling drive disease progression? Trends Mol Med 2008; 14:103–8.

[41] Zhu YB, Kang K, Zhang Y, Qi C, Li G, Yin DM, et al. PLD1 negatively regulates dendritic branching. J Neurosci 2012;32:7960–9.

[42] Luo L-D, Li G, Wang Y. PLD1 promotes dendritic spine development by inhibiting ADAM10-mediated N-cadherin cleavage. Sci Rep 2017; 7:6035.

[43] Musardo S, Marcello E, Gardoni F, Di Luca M. ADAM10 in synaptic physiology and pathology. Neurodegener Dis 2014;13:72–4.

[44] Saadipour K, Yang M, Lim Y, Georgiou K, Sun Y, Keating D, et al. Amyloid beta(1)(-)(4)(2) (Abeta(4)(2)) up-regulates the expression of sortilin via the p75(NTR)/RhoA signaling pathway. J Neurochem 2013;127:152–62.

[45] Du G, Altshuller YM, Kim Y, Han JM, Ryu SH, Morris AJ, et al. Dual requirement for rho and protein kinase C in direct activation of Phospholipase D1 through G protein-coupled receptor signaling. Mol Biol Cell 2000;11:4359–68.

[46] Ammar MR, Thahouly T, Hanauer A, Stegner D, Nieswandt B, Vitale N. PLD1 participates in BDNF-induced signalling in cortical neurons. Sci Rep 2015;5:14778.

[47] Han L, Stope MB, de Jesus ML, Oude Weernink PA, Urban M, Wieland T, et al. Direct stimulation of receptor-controlled phospholipase D1 by phospho-cofilin. EMBO J 2007;26:4189–202.

[48] Rudge SA, Wakelam MJ. Inter-regulatory dynamics of phospholipase D and the actin cytoskeleton. Biochim Biophys Acta 2009;1791:856–61.